William R. Wiley
EMSL
Environmental Molecular Sciences Laboratory

EMSL Report

July – September 2006

The W.R. Wiley Environmental Molecular Sciences Laboratory (EMSL) is a U.S. Department of Energy (DOE) national scientific user facility located at Pacific Northwest National Laboratory (PNNL) in Richland, Washington. EMSL is operated by PNNL for the DOE Office of Biological and Environmental Research (BER). At one location, EMSL offers a comprehensive array of leading-edge resources in six research facilities.

Access to the capabilities and instrumentation in EMSL facilities is obtained on a peer-reviewed proposal basis. Users are participants on accepted proposals. Staff members work with users to expedite access to the facilities and scientific expertise. This report documents research and activities of EMSL staff and users during the period from July through September 2006.

Research Highlights

Pb_{12}^{2-}: Plumbaspherene

LF Cui,[(a)] X Huang,[(a)] LM Wang,[(a)] J Li,[(b)] and LS Wang[(a)]
(a) Washington State University Tri-Cities, Richland, Washington
(b) W.R. Wiley Environmental Molecular Sciences Laboratory, Richland, Washington

Clusters are small groups of atoms that often have different properties than their corresponding bulk materials. In this work, the research team discovered a new class of endohedreal lead-cage compounds that they have named "plumbaspherenes." The existence of these new cage compounds may allow for the insertion of other atoms inside of these cages to create new materials with unique properties for a wide range of applications.

During recent photoelectron spectroscopy (PES) experiments aimed at understanding the semiconductor-to-metal transition in tin clusters, we found the spectra of Sn_{12}^- to be remarkably simple and totally different from the corresponding Ge_{12}^- cluster. This observation led to the discovery of a C_{5V} cage structure for Sn_{12}^-, which is only slightly distorted from the icosahedral (Ih) symmetry as a result of the Jahn-Teller effect. However, adding an electron to Sn_{12}^- resulted in a highly stable and closed-shell I_h Sn_{12}^{2-} cage cluster. Because of the large 5p-5s energy separation, the I_h Sn_{12}^{2-} cage was found to be bound primarily by the $5p^2$ electrons, which form four radial π bonds and nine in-sphere σ bonds, with the $5s^2$ electrons behaving like lone pairs. The Sn_{12}^{2-} cage was shown to be iso-electronic to the well-known $B_{12}H_{12}^{2-}$ molecule with the $5s^2$ lone pairs replacing the localized B-H bonds, and was named "stannaspherene" for its π-bonding characteristics and high symmetry.

In this highlight, we report both experimental and theoretical evidence that the corresponding Pb_{12}^{2-} cluster also exists as a highly stable I_h cage that has an even larger interior volume than stannaspherene and can host most transition metal atoms in the periodic table to form a new class of endohedral cage clusters.

Experimental evidence was obtained with a PES apparatus consisting of a laser vaporization supersonic cluster beam source and a magnetic bottle electron analyzer. Figure 1 shows the

PES spectra of Pb_x^- (x = 11-13) at 193 nm. Clearly, the Pb_{12}^- spectrum is special relative to those of its neighbors, showing only four bands (i.e., the X, A, B, and C bands), whereas much more complex spectral features are observed for Pb_{11}^- and Pb_{13}^-. This observation suggests that Pb_{12}^- should possess a relatively high symmetry structure. The current experimental data are better resolved spectra, have more accurate electron binding energies, and have more spectral features to cover the valence spectral range. As such, useful insights into these experimental results can be obtained from high-quality *ab initio* quantum mechanical calculations.

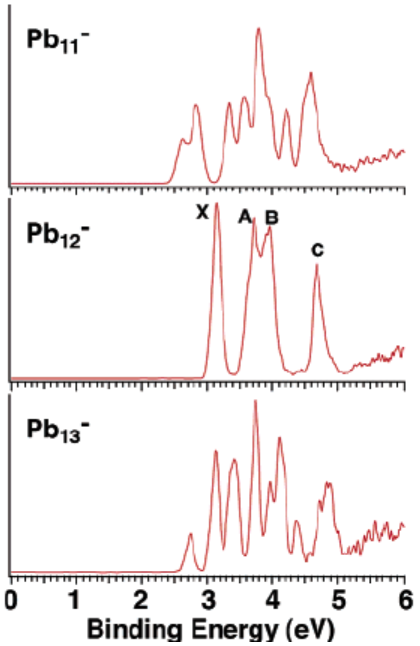

Figure 1. Photoelectron spectra of Pb_x^- (x = 11-13) at 193 nm. Note the relatively simple spectral pattern of Pb_{12}^- with respect to those of Pb_{11}^- and Pb_{13}^-.

Results of these calculations are shown in Figure 2. Geometry optimization for Pb_{12}^- from a high-symmetry icosahedral cage led to a Jahn-Teller distorted lower symmetry C_{5V} ($^2A_1$) species (Figure 2a) that is analogous to Sn_{12}^-. The computed first vertical detachment energy (3.08 eV) of the C_{5V} Pb_{12}^- is in excellent agreement with the experimental value of 3.14 eV. Whereas ion mobility experiments suggest that Pb_x^+ clusters possess compact near-spherical morphologies, several theoretical studies have given various structures for neutral Pb_{12}. However, we find that the doubly charged Pb_{12}^{2-} species is a highly stable and a perfect I_h cage with a closed electron shell (Figure 2b). Analogous to Sn_{12}^{2-}, which has been named stannaspherene for its π-bonding characteristics and its nearly spherical structure, we suggest the name "plumbaspherene" for the highly stable and robust Pb_{12}^{2-} cage. As such, we expect that the Pb_{12}^{2-} plumbaspherene should also be a stable species in solution and can be synthesized in the condensed phase. Plumbaspherene has a computed diameter of 6.29 Å, which is slightly larger than that of stannaspherene (6.07 Å). Thus, it is expected that Pb_{12}^{2-} can trap an atom inside its cage to form endohedral plumbaspherenes, M@Pb_{12}.

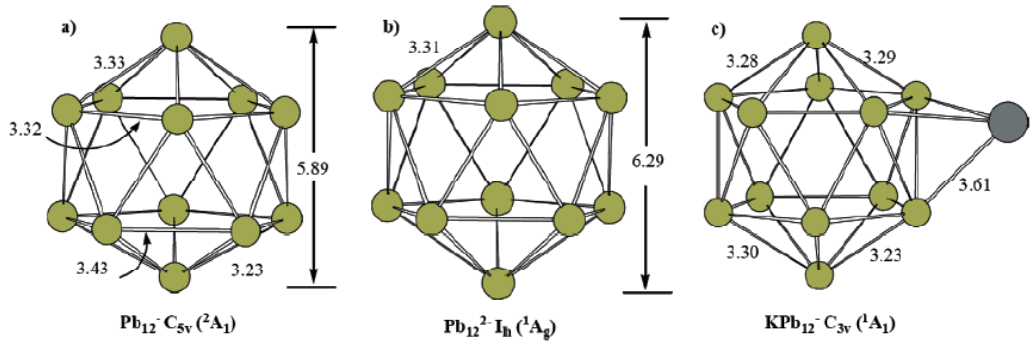

Figure 2. Optimized structures: (a) Pb_{12}^-, (b) Pb_{12}^{2-}, and (c) KPb_{12}^-. The bond distances and cage diameters are in Å.

We expect that a whole new family of stable M@Pb_{12} endohedral clusters may exist, analogous to the endohedral fullerenes. The plumbaspherene cages may be able to host a variety of transition metal atoms, thus creating a new class of endohedral cage clusters. Varying the host metal inside an M@Pb_{12} cage may dramatically change the properties of the cluster, thereby allowing the clusters to be tailored for specific applications. This exciting work was featured on the cover of the August 31, 2006, issue of *The Journal of Physical Chemistry A* (Figure 3).

Figure 3. Plumbaspherence shown on the cover of the *Journal of Physical Chemistry A*.

Citation

Cui LF, X Huang, LM Wang, J Li, and LS Wang. 2006. "Pb_{12}^{2-}: Plumbaspherene." *Journal of Physical Chemistry A* 110(34):10169-10172.

Solution Structure of the Complex Between Poxvirus-Encoded CC Chemokine Inhibitor vCCI and Human MIP-1ß

L Zhang,[(a)] M DeRider,[(b)] MA McCornack,[(c)] SC Jao,[(d)] NG Isern,[(e)] T Ness,[(f)] R Moyer,[(g)] and PJ LiWang[(a)]

(a) Texas A&M University, College Station, Texas
(b) Cardinal Health, Morrisville, North Carolina
(c) Promega Corporation, Madison, Wisconsin
(d) Academia Sinica, Nankang, Taipei, Taiwan
(e) W.R. Wiley Environmental Molecular Sciences Laboratory, Richland, Washington
(f) University of Michigan Medical Center, Ann Arbor, Michigan
(g) University of Florida, Gainesville, Florida

The chemokine system is critical for host defense in healthy individuals, but it also can lead to inflammatory diseases including asthma, arthritis, and atherosclerosis. This novel work used high-field nuclear magnetic resonance (NMR) spectroscopy to reveal the first known structure of a 35-kDa pox virus chemokine inhibitor:human chemokine complex, which is a stepping stone to future therapeutic drug design.

Chemokines (i.e., chemotactic cytokines) comprise a large family of proteins that recruit and activate leukocytes, giving chemokines a major role in both immune response and inflammation-related diseases. To date, about 50 chemokines have been identified, and these small proteins (7 to 14 kDa) are believed to function by binding with endothelial or matrix glycosaminoglycans (GaGs) to form a concentration gradient that is then sensed by high-affinity, 7-transmembrane domain G-protein coupled chemokine receptors on the surface of immune cells, leading to activation and chemotaxis. Chemokines play critical roles in the immune system, causing chemotaxis of a variety of cells to sites of infection and inflammation, as well as mediating cell homing and immune system development (Baggiolini 2001; Gerard and Rollins 2001). There are four subfamilies of chemokines, CC, CXC, C, and CX_3C, which are named for the position of conserved N-terminal cysteine residues; different subfamilies tend to function on different cell subsets (Baggiolini 2001).

All known pox and herpes viruses encode proteins that interfere with the host chemokine network, probably as part of a strategy to manipulate and subvert the immune system (Boomker et al. 2005). Such virally encoded proteins include chemokine mimics, chemokine receptor analogs, and a group of secreted, soluble chemokine binding proteins (CKBPs) that exhibit little similarity to any mammalian protein (Seet and McFadden 2002). CKBPs competitively bind to chemokines and disrupt chemokine interactions with the host cell surface receptors or GAGs. Although some CKBPs interact with a very broad spectrum of chemokines across several chemokine subfamilies, the poxvirus-encoded viral CC chemokine inhibitor (vCCI) proteins bind selectively to the CC family of pro-inflammatory chemokines (Seet and McFadden 2002; Lalani et al. 1998). The vCCI proteins have been shown to be potent inhibitors of chemokine action *in vitro* (Lalani et al. 1998) and effective anti-inflammatory agents in vivo (Dabbagh et al. 2000).

Figure 1. Solution structure of the vCCI:MIP-1β complex, with vCCI backbone in green and MIP-1β backbone in violet.

Although the structures of several chemokines (Clore et al. 1990; Mayer and Stone 2000; Crump et al. 1997; Fernandez and Lolis 2002), as well as the individual structure of vCCI (11) are known, no structure had previously been solved of a vCCI:chemokine complex, so the structural basis of vCCI's interaction with chemokines was not clear. We have used heteronuclear multidimensional NMR to determine the first structure of an orthopoxvirus vCCI in complex with a human CC chemokine MIP-1ß variant. Access to high-field spectrometers at the EMSL High-Field Magnetic Resonance Facility was critical to obtaining the spectral data that enabled structure determination work on this 35-kDa complex.

Our structural studies reveal that the vCCI and MIP-1ß form a complex in a 1:1 stoichiometry, and that vCCI occludes the regions in the chemokine that are important for chemokine homo-dimerization, receptor binding, and glycosaminoglycan interaction (Figure 1). The structure also defines key interactions that form the basis for the affinity and selectivity of vCCI towards certain CC chemokines. The insights gained from this groundbreaking work will be critical to development of therapeutic agents to modulate immune response. This work was published in *Proceedings of the National Academy of Sciences of the United States of America* in September 2006.

Citations

Baggiolini M. 2001. "Chemokines in Pathology and Medicine." *Journal of Internal Medicine* 250(2):91-104.

Boomker JM, LF de Leij, TH The, and MC Harmsen. 2005. "Viral Chemokine-Modulatory Proteins: Tools and Targets." *Cytokine & Growth Factor Reviews* 16(1):91-103.

Clore GM, E Appella, M Yamada, K Matsushima, and AM Gronenborn. 1990. "Three-Dimensional Structure of Interleukin 8 in Solution." *Biochemistry* 29(7):1689-1696.

Crump MP, JH Gong, P Loetscher, K Rajarathnam, A Amara, F Arenzana-Seisdedos, JL Virelizier, M Baggiolini, B Sykes, and I Clark-Lewis. 1997. "Solution Structure and Basis for Functional Activity of Stromal Cell-Derived Factor-1; Dissociation of CXCR4 Activation from Binding and Inhibition of HIV-1." *EMBO Journal* 16(23):6996-7007.

Dabbagh K, Y Xiao, C Smith, P Stepick-Biek, SG Kim, WJ Lamm, DH Liggitt, and DB Lewis. 2000. "Local Blockade of Allergic Airway Hyperreactivity and Inflammation by the Poxvirus-Derived Pan-CC-Chemokine Inhibitor vCCI." *Journal of Immunology* 165(6):3418-3422.

Fernandez EJ and E Lolis. 2002. "Structure, Function, and Inhibition of Chemokines." *Annual Review of Pharmacology and Toxicology* 42:469-499.

Gerard C and BJ Rollins. 2001. "Chemokines and Disease." *Nature Immunology* 2(2): 108-115.

Lalani AS, TL Ness, R Singh, JK Harrison, BT Seet, DJ Kelvin, G McFadden, and RW Moyer. 1998. "Functional Comparisons among Members of the Poxvirus T1/35-kDa Family of Soluble CC-Chemokine Inhibitor Glycoprotei." *Virology* 250(1):173-184.

Mayer KL and MJ Stone. 2000. "NMR Solution Structure and Receptor Peptide Binding of the CC Chemokine Eotaxin-2." *Biochemistry* 39(29):8382-8395.

Seet BT and G McFadden. 2002. "Viral Chemokine-Binding Proteins." *Journal of Leukocyte Biology* 72(1):24-34.

Reductive Biotransformation of Iron in Shale-Limestone Saprolite Containing Fe(III) Oxides And Fe(II)/Fe(III) Phyllosilicates

R Kukkadapu,[(a)] JM Zachara,[(b)] J K Fredrickson,[(b)] JP McKinley,[(b)] DW Kennedy,[(b)] SC Smith,[(b)] and H Dong[(c)]

(a) W.R. Wiley Environmental Molecular Sciences Laboratory, Richland, Washington

(b) Pacific Northwest National Laboratory, Richland, Washington

(c) Miami University, Oxford, Ohio

Iron reduction by dissimilatory metal-reducing bacteria is an important process in anoxic soils, sediments, and subsurface materials, particularly for bioremediation applications. However, the bioavailability of mineral Fe(III) to metal-reducing bacteria appears limited by numerous incompletely understood factors, such as crystal chemistry, solid-phase thermodynamics and surface area effects, and electron transfer efficiency at the mineral-microbe interface.

In this study, we used Mössbauer spectroscopy to determine 1) the distribution of Fe(III) and Fe(II) between mineral sites and between mineral phases prior to and following microbial reduction and 2) the fate of biogenic Fe(II). Mössbauer measurements on the bioreduced sediments indicated that both goethite and phyllosilicate Fe(III) were partially reduced. Biogenic Fe(II) resulting from phyllosilicate Fe(III) reduction remained in a layer-silicate environment that displayed enhanced solubility in weak acid (Figure 1). The mineralogic nature of the goethite biotransformation product could not be identified but was determined not to be siderite, green rust, magnetite, $Fe(OH)_2$, or Fe(II) adsorbed on phyllosilicate or bacterial surfaces. Several lines of evidence suggested that biogenic Fe(II)

existed as surface-associated phase on the residual goethite, and/or as a Fe(II)-Al co-precipitate. The results of this work were published in the journal *Geochimica et Cosmochimica Acta* (Kukkapadu et al. 2006).

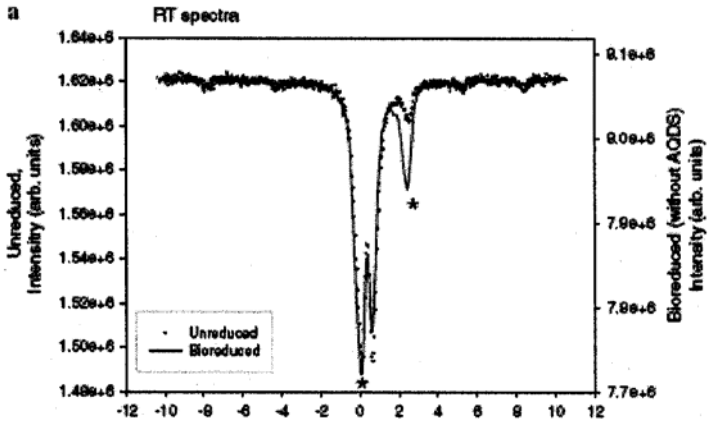

Figure 1. Mössbauer spectra of unreduced and bioreduced sediment.

Citation

Kukkadapu RK, JM Zachara, JK Fredrickson, JP McKinley, DW Kennedy, SC Smith, and HL Dong. 2006. "Reductive Biotransformation of Fe in Shale-Limestone Saprolite Containing Fe(III) Oxides and Fe(II)/Fe(III) Phyllosilicates." *Geochimica et Cosmochimica Acta* 70(14):3662-3676.

Proteomic Profiling of *Corynebacterium glutamicum* R Incubated at Very High Cellular Densities Under Oxygen-Deprivation Conditions

S Okino,[(a)] CA Omumasaba,[(a)] M Suda,[(a)] M Inui,[(a)] AA Vertès,[(a)] MS Lipton,[(b)] SO Purvine,[(c)] TR Clauss,[(b)] and H. Yukawa[(a)]

(a) Research Institute of Innovative Technology for the Earth, Kyoto, Japan

(b) Pacific Northwest National Laboratory, Richland, Washington

(c) W.R. Wiley Environmental Molecular Sciences Laboratory, Richland, Washington

The completion of the human genome dramatically showed that there are not enough genes available to account for the diversity and complexity that we have. Thus, it is the regulation of the translation of the genome into proteins that leads to this diversity and this regulation is one of the great unsolved problems in biology. Analysis of the proteins in simpler model systems like Corynebacterium glutamicum R *will give us insights into how this regulation is controlled.*

The recent completion of the genome sequence of *Corynebacterium glutamicum* R enables the implementation of post-genomic tools to define the physiological response exhibited by this microorganism when it is subjected to various environmental conditions. We have established and validated basic procedures for performing comparative proteomic profiles of *Corynebacterial* protein extracts. We observed a general agreement between proteomics and transcriptomics data. Further analyses could possibly reveal in this organism the presence of unknown regulatory mechanisms and global metabolic adaptations that occur when the culture is switched from the cell catalyst production phase to the product production phase.

In the quest for cost-effective production processes that would be suitable for producing a variety of commodity chemicals, such as ethanol or organic acids, the Research Institute of Innovative Technology for the Earth in Kyoto, Japan, has championed the development of novel processes that make use of very high cellular densities and oxygen-deprivation conditions. These conditions trigger the uncoupling of cell catalyst production and product production phases in anaero-tolerant and quorum-sensing sensitive organisms (Inui et al.

2004a, b; Inui et al. 2006). The complete genomic sequences of *C. glutamicum* R and *C. glutamicum* ATCC 13032 (Yukawa et al. 2006) enable us to use post-genomic tools for the global analysis of the cellular responses that *C. glutamicum* exhibits when subjected to various incubation conditions. Particularly, two-dimensional poly-acrylamide gel electrophoresis (2D-PAGE) combined to liquid chromatography/mass spectrometry (LC/MS) of *C. glutamicum* R protein extracts enabled to identify numerous enzymes of the central metabolism (Figure 1).

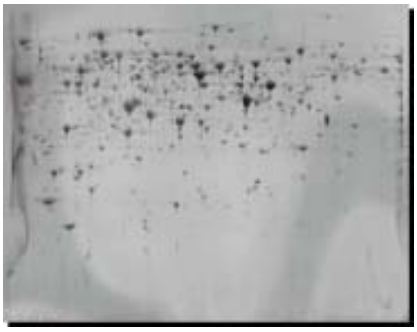

Figure 1. Two-dimensional poly-acrylamide gel electrophoresis imaging of *C. glutamicum* R protein extracts. Numerous proteins could be identified by LC/MS analysis, including key enzymes of the central metabolism (e.g., enolase, transketolase, fumarase, acetyl-CoA hydrolase, pyruvate kinase, malate dehydrogenase, glyceraldehyde-3-phosphate dehydrogenase, fructose-biphosphate aldolase, triosephosphate isomerase, and fructose-1,6-biphosphatase).

Moreover, global transcriptomics analyses unraveled the genetic expression patterns in *C. glutamicum* R incubated under very high cellular densities and then subjected to oxygen deprivation (Figure 2).

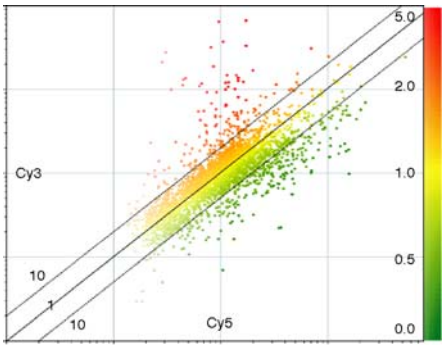

Figure 2. Scatter plot of log Cy3- and log Cy5-derived fluorescence. Each dot represents the average of six independent experiments. The RNA of *C. glutamicum* R cells grown under aerobic conditions and of similarly grown cells but reacted under process conditions was used for Cy3 and Cy5 labeling. The two outer dotted lines demarcate values for significant differences in gene expression levels (i.e., by factors of two and one-half).

While global transcriptional profiling constitutes an extremely useful technique for optimizing manufacturing strains by rational design, its main limitation is that it does not provide any relevant information regarding constitutively expressed genes or regarding those metabolic nodes that are regulated at the protein-modification level. In addition, transcriptome analysis cannot account for differential transcript stability, thus making the relationship between mRNA abundance and protein activity unclear for numerous enzymes (Yukawa et al. 2006). As a result, we applied mass spectroscopy techniques to trypsin-digested protein extracts of *C. glutamicum* R to attain both quantitative and qualitative data, in an effort to document the variations of the protein content of this organism. Specifically, we measured the relative abundance of several peptides per protein, thus uniquely characterizing that protein. This redundancy in data is important because it enables us to achieve higher data robustness. Beyond providing a complete list of such unique signature peptides, we compared the relative abundance of various proteins among samples including extracts representing protein soluble fractions, insoluble fractions, and total proteins. These fractions were isolated from both exponentially growing cells and from cells incubated under production conditions (very high cellular densities, oxygen-deprivation). As expected, a general tendency toward agreement between transcriptomic and proteomic data was observed (Figure 3).

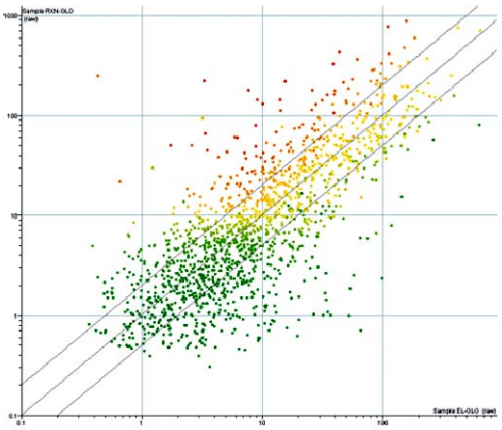

Figure 3. Scatter plot of relative protein abundance as measured by mass spectrometry of trypsin digests of total protein extracts recovered from exponentially growing cells (x axis), and from cells incubated under process conditions (y axis). The two outer dotted lines demarcate values for significant differences in protein levels (i.e., by factors of two and one-half).

This initial set of data demonstrates the robustness of the method employed, including the protein extract preparation method, and thus paves the way to detailed analyses of 1) the global metabolism of *C. glutamicum* and 2) the dynamic regulatory networks that regulate it. Furthermore, the various unique signature peptides identified in the course of these experiments will enable the study of very short proteins synthesized by *C. glutamicum*, and thus contribute significantly to enhancing the quality of the annotation of the *C. glutamicum* R and *C. glutamicum* ATCC 13032 genomes.

Citations

Inui M, H Kawaguchi, S Murakami, AA Vertès, and H Yukawa. 2004a. "Metabolic Engineering of *Corynebacterium glutamicum* for Fuel Ethanol Production Under Oxygen-Deprivation Conditions." *Journal of Molecular Microbiology and Biotechnology* 8(4):243-254.

Inui M., S Murakami, S Okino, H Kawaguchi, AA Vertès, and H Yukawa. 2004b. "Metabolic Analysis of *Corynebacterium glutamicum* During Lactate and Succinate Productions Under Oxygen Deprivation Conditions." *Journal of Molecular Microbiology and Biotechnology* 7(4):182-196.

Inui, M, AA Vertès, S Okino, K Iwasaki, S Sakai, T Watanabe, and H Yukawa. 2006. "Growth-Independent Bioprocess for Ethanol Production Using *Corynebacterium glutamicum*." *Applied Microbiology and Biotechnology* in press.

Yukawa, H, M Inui, and AA Vertès. 2006. "Genomes and Genome Level Engineering of Amino Acid Producing Bacteria." In *Amino Acid Biosynthesis–Pathways, Regulation, and Metabolic Engineering*, ed. V. F. Wendisch, Springer, Heidelberg, Germany.

Optimum Conductivity in Oriented $[Ce_{0.89}Sm_{0.11}]O_{2-x}$ Thin Films Grown by Oxygen-Plasma-Assisted Molecular Beam Epitaxy

ZQ Yu,[(a)] LV Saraf,[(b)] OA Marina,[(c)] CM Wang,[(b)] MH Engelhard,[(b)] V Shutthanandan,[(b)] P Nachimuthu,[(b)] DE McCready,[(b)] and S. Thevuthasan[(b)]

(a) Nanjing Normal University, Nanjing, China

(b) W.R. Wiley Environmental Molecular Sciences Laboratory, Richland, Washington

(c) Pacific Northwest National Laboratory, Richland, Washington

Investigations in alternative and clean energy technology have become essential to reduce the dependence on more traditional energy resources. Solid oxide fuel cells (SOFC) provide such clean energy without hazardous by-products. The research described in this highlight is motivated by the use of epitaxial Sm:CeO_2 as a potential electrolyte material in SOFC. In this study, we have observed high conductivity values in epitaxial Sm:CeO_2 films.

Development of electrolyte materials that possess high oxygen ion conductance at relatively low temperatures is essential to increase the efficiency and lifetime of SOFC. Lower operating temperatures would make SOFCs more cost efficient and could facilitate their use in broader applications. At lower operating temperatures, SOFCs could also avoid many undesirable interfacial reactions between electrodes and electrolyte materials. In this study, we used molecular-beam epitaxy, which enables precise growth control, to grow SOFC electrolyte layers. Oriented electrolyte layers, such as Sm:CeO_2, can potentially provide higher conductivity through a reduction in grain-boundary density, thus avoiding the unnecessary scattering across a layer. Sm:CeO_2 films were grown on single crystal c-Al_2O_3 in a dual-chamber, ultrahigh-vacuum system equipped with an electron cyclotron resonance oxygen plasma source. After the surface plasma cleaning at 600°C, films were grown at simultaneous growth rates of 0.2 and 0.01 nm/s for cesium and samarium, respectively, in an oxygen partial pressure of ~2.0×10^{5} Torr and at a substrate temperature of 650°C. Cesium (99.98 percent purity) and samarium (99.98 percent purity) were evaporated from an e-bam source and an effusion cell, respectively. The growth rates of the films were monitored by quartz crystal oscillators (QCOs). The *in situ* film growth was monitored using reflection high-energy electron diffraction.

X-ray photoelectron spectroscopy (XPS) depth profiles give excellent overviews of the atomic elemental concentrations of cesium, samarium, oxygen, and aluminum as a function of film depth. Figure 1 shows the XPS depth profile in the case of 5 atom% Sm:CeO_2 film. A uniform samarium concentration as a function of film depth was noted, and $Ce_{0.89}Sm_{0.11}O_{2-x}$ was determined

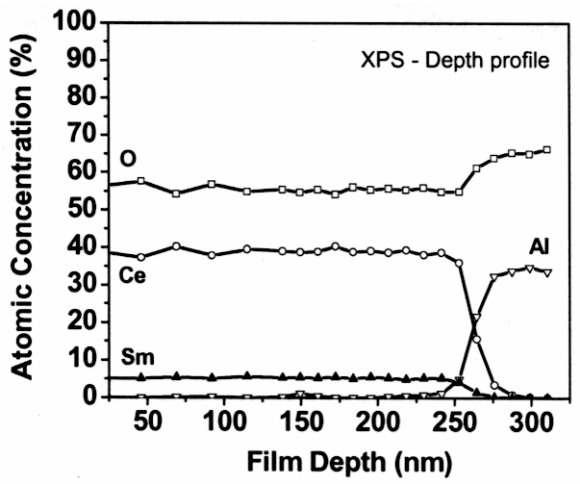

Figure 1. The XPS depth profile of 5 atom% Sm:CeO_2 film on c-Al_2O_3. A uniform samarium concentration throughout the film with surface oxygen enhancement can also be seen in the data.

to be the stoichiometry of the film. In addition, a fairly sharp interface between Sm:CeO_2 and Al_2O_3 was also realized from the spectra. Four-probe conductivity measurements were done on Sm:CeO_2 films with samarium concentration in the range of 1 to 23 atom%. Figure 2 shows Arrhenius plots of Sm:CeO_2 films with various samarium atomic concentrations in the measurement temperature range of 500 to 900°C. The figure shows that film with a 5 atom% samarium concentration shows maximum conductivity compared to other doping concentrations. We concluded that a loss of (111) orientation enhances the grain boundary scattering, thereby reducing the conductivity. However, our observed conductivity of 0.04 $S.cm^{-1}$ at 600°C is one of the highest conductivities observed in these materials. The activation energy E_a, derived from the slope of the Arrhenius plot, is observed at 0.86 eV for the as-grown films. Typically lower activation energy refers to lower barrier for the oxygen transport throughout the Sm:CeO_2 crystal.

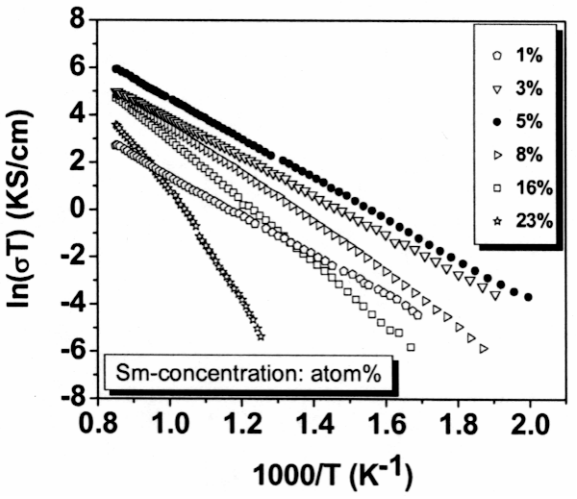

Figure 2. Arrhenius plots of Sm:CeO_2 films with various samarium atomic concentrations in the measurement temperature range of 500 to 900°C.

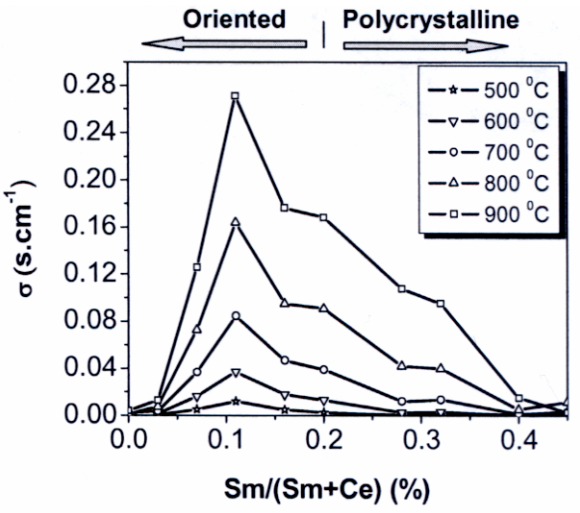

Figure 3. The conductivity of Sm:CeO_2 as a function of samarium concentration in the range of 1-23 atom% at measurement temperatures from 500 to 900°C. At all measurement temperatures, highest conductivity is seen at 5 atom% samarium concentration.

Figure 3 shows the conductivity of Sm:CeO_2 as a function of Sm/(Sm+Ce) for the samarium concentration range of 1 to 23 atom%. The variation in conductivity as a function of temperature with different samarium concentrations is seen to get narrower at lower and higher samarium concentrations. The dopant saturation is likely to cause narrower conductivity variation at the higher samarium concentrations end, whereas limited dopant incorporation is primarily responsible for narrower variation at lower samarium concentrations.

Thermal Oxidation of Aluminum Nitride Powder

Z Gu,[(a)] JH Edgar,[(a)] CM Wang,[(b)] and DS Coffey[(c)]
(a) Kansas State University, Manhattan, Kansas
(b) W.R. Wiley Environmental Molecular Sciences Laboratory, Richland, Washington
(c) Pacific Northwest National Laboratory, Richland, Washington

The goal of this study was to determine and compare the oxidation behavior of two types of aluminum nitride (AlN) powder with different morphology and particle sizes. The kinetics of oxidation, the properties of the formed aluminum oxide layer, and the morphology change before and after oxidation were studied in detail using a combination of x-ray diffraction analysis and tunneling electron microscopy.

Aluminum nitride has a good thermal stability (melting point >2750°C), high thermal conductivity (3.2 W/cm·K) and electrical resistivity (>4 × 10^8 ohm·cm), and a low dielectric constant (9 at 1 MHz) and coefficient of thermal expansion (4.03-6.09 × 10^{-6}/K). Therefore, AlN has been widely used in the electronic and optoelectronic areas. Oxygen, a common impurity in AlN, has a detrimental effect on its properties: it reduces the lattice parameters of AlN and remarkably decreases its thermal conductivity. Therefore, understanding how oxygen enters the AlN lattice constitutes an important step for understanding the oxidation process. For example, a native oxide film of 5 to 10 nm in thickness is obtained following exposing AlN in air for 24 hours at room temperature. This initial oxide layer is protective and prevents further oxidation.

In general, three sequential steps occur during the thermal oxidation of most materials, one of which may be the rate-limiting step. First, the oxidant (typically oxygen or water vapor) transports in the gas phase to the oxide surface. Second, the oxidant diffuses through the oxide layer to the substrate/oxide interface. Third, and finally, the oxidation reaction occurs at the interface. The diffusion process in the gas phase is usually very fast compared to the other two steps, thus it is insignificant in determining the overall growth kinetics. Initially, when the oxide layer is thin, the oxidant quickly transports through the oxide to the interface to sustain the chemical reaction, hence the whole process is controlled by the interfacial reaction. As the oxide layer thickness increases, the diffusion of the oxidant through the oxide layer slows and becomes the rate-limiting step in the overall process. The thermal oxidation of silicon is a typical example of the three-step process. However, in the thermal oxidation of AlN, which is governed by the overall reaction $2AlN + 1.5O_2 \leftrightarrow Al_2O_3 + N_2$, the out-diffusion of product gas nitrogen through the oxide film and the removal of nitrogen away from the oxide surface are two additional steps that are not involved in the oxidation of silicon. The latter step is usually rapid and is not a rate-controlling step.

Two types of AlN powder were oxidized in flowing oxygen over the temperature range from 800 to 1150°C. For a Type-A AlN powder (average agglomerated particle size 1.8 μm), oxidation began above 900°C after 6 hours and was almost complete at 1050°C, but only for 30 minutes. Crystalline Al_2O_3 formed above 1050°C, while amorphous Al_2O_3 or oxynitrides formed at lower temperatures. The oxidation of Type-A AlN powder was a linear reaction over time between 800 and 1000°C, and the activation energy was 157.2 kJ/mol. These conditions indicated that an interfacial reaction governed the process. At temperatures higher than 1000°C (1050, 1100, and 1150°C), approximately 95 percent of the AlN was oxidized after only 30 minutes, and the conversion barely changed with further increases in the oxidation temperature or time. For a Type-B AlN powder (particle size 14.0 to 23 μm), oxidation became observable at 800°C after 6 hours, and the oxidation extent was higher

than that of Type-A AlN powder at temperatures ranging from 800 to 1000°C. The oxidation kinetics changed from linear in the 800 to 900°C temperature range to parabolic in the 1000 to 1150°C range, suggesting that control of the process changed from interfacial reaction control to oxidant diffusion control. The complex oxidation difference observed between the two AlN powder types was probably caused by the different morphologies of the powders, and by their different particle sizes, particle-size distributions, and impurities. Figure 1 shows transmission electron microscopy images of oxidized AlN particles, revealing a pore trapped in a particle.

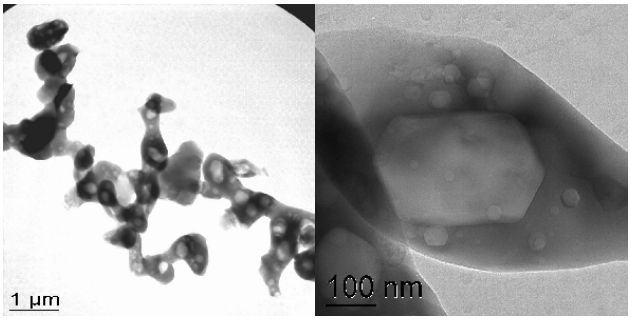

Figure 1. Transmission electron microscopy images of oxidized AlN particles, revealing a pore trapped in a particle.

Oxidation of AlN powders, sintered polycrystalline substrates, and thin films has been extensively investigated. Abid et al. (1986) found that AlN powder was resistant to oxidation in air up to ~1000°C. For AlN powder heated to 1000°C, an unidentified phase was detected by reflection high-energy electron diffraction, possibly an oxide or oxynitride. At 1200°C, the AlN was completely transformed to α-Al_2O_3. However, no differences were reported for the oxidation of AlN powders with different particle sizes. Brown et al. (1998) observed a linear weight increase of AlN powder over time when heated in air at 850°C. The activation energy was calculated to be 271 kJ/mol. At temperatures above 850°C, the weight change increased parabolically, and the activation energy was 423 kJ/mol, which agreed well with the 459 kJ/mol experimental value for the diffusion of oxygen through polycrystalline Al_2O_3. X-ray diffraction, scanning electron microscopy, and infrared spectroscopy were employed by Ramanthan et al. (1995) to study the oxidation behavior of AlN powder at temperatures in the 900 to 1150°C range. An initial linear kinetic regime with activation energies of 197 and 270 kJ/mol was observed. A poorly crystalline spinel-type aluminum oxynitride formed at 900°C. This phase was transformed into α-alumina crystallites at higher temperatures. The oxide morphology changed from a fine-grained and coherent structure at 950°C to a porous fissured structure at 1150°C.

In addition to oxidation temperature and time, the condition of the original AlN powder is crucial in determining the thermal oxidation behavior. Particle size and impurity concentration are two important parameters in describing AlN powder. The surface-area-to-volume ratio of small particles is typically much higher than that of large particles, leaving more surface area exposed per mass. Thus, small particles are expected to oxidize faster than larger particles. The effect of particle size on the AlN oxidation rate was examined by Suryanarayana (1990). The initially rapid oxidation rate decreased over time for a fine AlN powder with a mean particle radius and standard deviation of 0.5 µm and 1.6, respectively. In contrast, the oxidation rate was almost constant with time for a coarse powder with a mean particle radius and a standard deviation of 3.1 µm and 2.1, respectively. Highly doped silicon substrates oxidize more rapidly than lightly doped silicon wafers, and the difference in reaction rates is greater at lower temperatures or for thinner oxides. One possible explanation is that oxidation requires volume expansion that can be provided by the consumption of vacancies at the silicon/silicon dioxide interface.

An article describing this research was published in the July 2006 edition the *Journal of the American Ceramic Society* (Gu et al. 2006).

Citations

Abid A, R Bensalem, and BJ Shealy. 1986. "The Thermal Stability of AlN." *Journal of Materials Science* 21(4):1301-1304.

Brown AL and MG Norton. 1998. "Oxidation Kinetics of AlN Powder." *Journal of Materials Science* 17(18):1519-1522.

Gu Z, JH Edgar, CM Wang, and DW Coffey. 2006. "Thermal Oxidation of Aluminum Nitride Powder." *Journal of the American Ceramic Society* 89(7)2167-2171.

Ramanathan S, R Bhat, DD Upadhyaya, and SK Roy. 1995. "Oxidation Behavior of Aluminum Nitride Powder." *British Ceramic Transactions* 94(2):74-78.

Suryanarayana D. 1990. "Oxidation Kinetics of Aluminum Nitride Powders." *Journal of the American Ceramic Society* 73(4):1108-1110.

Study of Hydrogen Stability in Low-K Dielectric Films by Ion Beam Techniques

Y Zhang,[(a)] L Saraf,[(a)] V Shutthanandan,[(a)] KD Hughes,[(a)] R Kuan,[(b)] and S Thevuthasan[(a)]
(a) W.R. Environmental Molecular Sciences Laboratory, Richland, Washington
(b) Texas Instruments Incorporated, Dallas, Texas

With shrinking device geometries into the 65-nm technology node, a transition to low-k dielectrics becomes increasingly attractive. Negative bias temperature instability, which is associated with hydrogen migration at elevated temperatures, becomes the main degradation mechanism of concern for conductivity breakdown in semiconductor devices. The possibility of hydrogen release during each stage of the fabrication process is, therefore, of great interest to the understanding of device reliability. In this study, various low-k dielectric films were subjected to thermal annealing in a nitrogen atmosphere at temperatures that are generally used when fabricating devices. Rutherford backscattering spectrometry (RBS) and elastic recoil detection analysis (ERDA) were used to investigate composition changes and hydrogen redistribution of the dielectric films.

In interlayer dielectric (ILD) applications, plasma-enhanced tetraethylorthosilicate (PETEOS) films have been used to achieve better step coverage, especially for submicron gap spaces. With addition of phosphorus dopants during the deposition, phosphorus-doped silicon glass (PSG) films become viscous at elevated temperatures and respond to surface tension forces and the rounding of

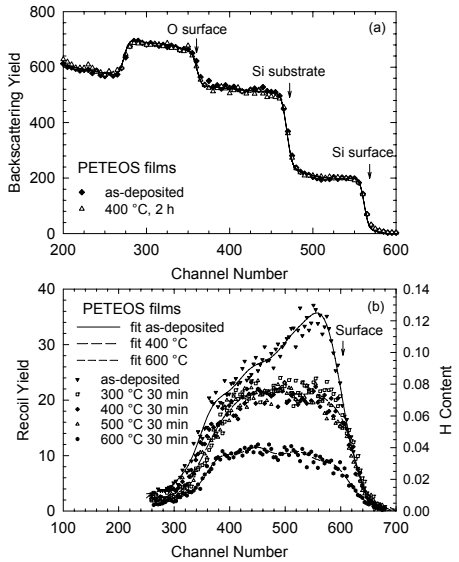

Figure 1. (a) RBS spectra of PETEOS films before and after 400°C for 2 hours; (b) ERDA spectra of the as-deposited PETEOS film and the films that are subjected to thermal treatments.

sharp corners, which is extremely useful in forming uniform doping inside gaps with high aspect ratios.

Furthermore, PSG films have an alkali ion-gettering capability, which makes it well suited for use as a passivation layer. In this project, the composition changes of the PETEOS and PSG films before and after annealing at 400°C for 2 hours were studied by RBS. The RBS spectra along with the simulated spectra are presented in Figures 1(a) and 2(a). In addition, hydrogen stability was investigated by measuring the total hydrogen in the films using conventional ERDA after the heat treatments up to 600°C, as shown in Figures 1(b) and 2(b). In the figures, higher hydrogen concentrations are observed in the surface regions of as-deposited PETEOS and PSG films. In the as-deposited films, the hydrogen concentration in the surface region consists of hydrogen from the films and from the hydrocarbon contamination on the film surfaces. After heat treatment up to 400°C for 2 hours, the main structures of both films are preserved. Significant hydrogen reductions at both the PETEOS and the PSG sample surfaces are observed after annealing at 300°C. Although the PETEOS films show some hydrogen reduction in the bulk of the film after this annealing, reduction of hydrogen is less significant in the bulk of the PSG films, indicating the existence of weakly bound hydrogen compounds in the bulk of the PETEOS films. After annealing at 400 and 500°C, no significant hydrogen reduction is observed in both films, and hydrogen is more uniformly distributed in the films, approximately 7.5 percent in the PETEOS films and 2.5 percent in the PSG films. As the annealing temperature increases to 600°C, both the PETEOS and PSG films decompose with significant hydrogen releases, and a SiO_2 film begins to form.

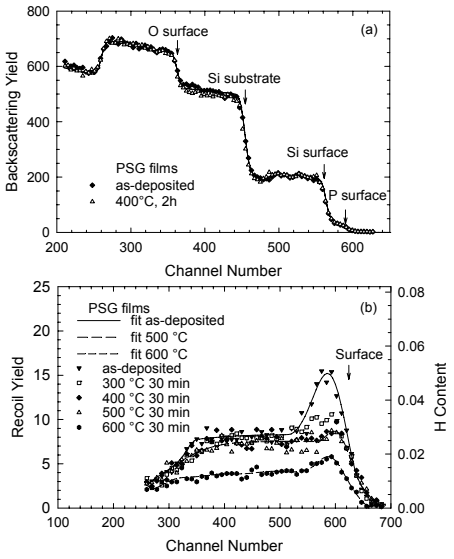

Figure 2. (a) RBS spectra of PSG films before and after 400°C for 2h. (b) ERDA spectra of the as-deposited and annealed PSG films.

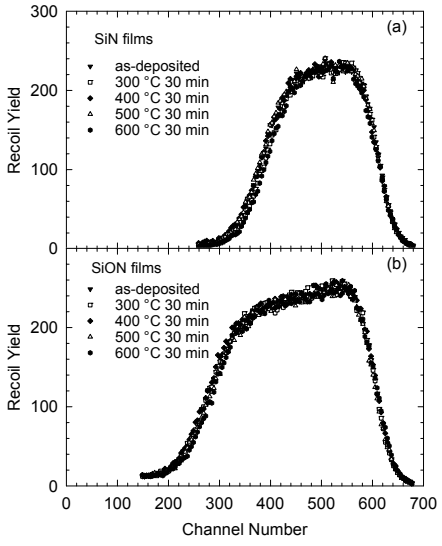

Figure 3. ERDA spectra of the as-deposited film and annealed (a) SiN films and (b) SiON films.

Silicon nitride (SiN) is a widely used dielectric material in very large-scale integration fabrication because of its impermeability to most impurities, such as a diffusion barrier to moisture, or as a selective oxidation mask to prevent oxygen from penetrating into the silicon underlayer. Silicon oxynitride (SiON) films, in which the composition changes

continuously from oxide to nitride by varying gas flow during plasma-enhanced chemical vapor deposition, demonstrate improved stability and better cracking resistance with low film stress. Thus, SiON films are considered to be unique materials for intermetal-level dielectric and final passivation layers. The SiN and SiON films are thermally stable up to 600°C annealing, (Figure 3). No hydrogen redistribution or structural changes are observed within the measurement uncertainties.

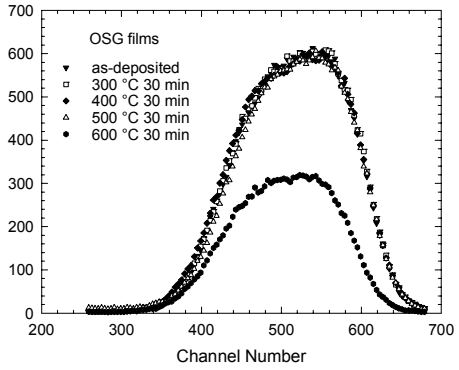

Figure 4. ERDA spectra of the as-deposited and thermally treated OSG films.

To further decrease the dielectric constant of the ILD layers as the device dimension decreases to sub-100-nm fields, introducing nanoscale pores into the dielectrics is an effective approach for meeting ultra-low-k demand. Among various porous low-k materials, organosilicate glass (OSG) films are promising candidates as ILD materials for high-performance interconnects. The OSG films used in this study were carbon-doped, low-k material with incorporated organic groups (e.g., $-CH_3$). No change was observed after heat treatment up to 400°C for 2 hours. ERDA results indicate that hydrogen bonds are stable up to 500°C for 30 minutes, as shown in Figure 4. However, release of hydrogen from the film during 600°C annealing is evident.

In this project, we investigated the stability of low-k dielectric films subjected to heat treatment up to 600°C. The results indicate that there is a significant hydrogen release from the surface region of the PETEOS and PSG films at 300°C and insignificant hydrogen releases in the temperature range from above 300°C to 500°C. The films start to decompose by releasing hydrogen at 600°C and form SiO_2. The SiN and SiON films are stable after heat treatment at 600°C for 30 minutes. Similar to the PETEOS and PSG films, the OSG films are stable up to 500°C and then break down at 600°C.

ScalaBLAST: A Scalable Implementation of BLAST for High-Performance, Data-Intensive Bioinformatics Analysis

CS Oehmen[(a)] and J Nieplocha[(a)]
(a) Pacific Northwest National Laboratory, Richland, Washington

Developers at PNNL have developed ScalaBLAST, a high-performance, sequence-alignment application that accommodates very large databases and scales linearly to hundreds of processors on both distributed memory and shared memory architectures. This new software represents a substantial improvement over the current state of the art in high-performance sequence alignment with scaling and portability and should have wide-ranging application to other informatics-driven sciences.

Genes in an organism's DNA (genome) have embedded in them information about proteins, which are the molecules that do most of a cell's work. A typical bacterial genome contains on the order of 5000 genes. Mammalian genomes can contain hundreds of thousands of genes. For each genome sequenced, the challenge is to identify protein components (i.e., proteomes) being actively used for a given set of conditions. Fundamentally, sequence

alignment is a sequence-matching problem that focuses on unlocking protein information embedded in the genetic code, making it possible to assemble a "tree of life" by comparing new sequences against all sequences from known organisms. However, the memory footprint of sequence data is growing more rapidly than per-node core memory. Despite years of research and development, high-performance, sequence-alignment applications do not scale well, cannot accommodate very large databases, or require special hardware. To solve these propblems PNNL researchers developed ScalaBLAST, a high-performance, sequence-alignment application that accommodates very large databases and scales linearly to hundreds of processors on both distributed memory and shared memory architectures (see Figure 1). ScalaBlast represents a substantial improvement over the current state of the art in high-performance sequence alignment with scaling and portability. It relies on a collection of innovative techniques (e.g., target database distribution over available memory, multi-level parallelism to exploit concurrency, parallel input/output, and latency hiding through data pre-fetching) to achieve high performance and scalability. This demonstrated approach of database sharing combined with effective task scheduling should have wide-ranging application to other informatics-driven sciences.

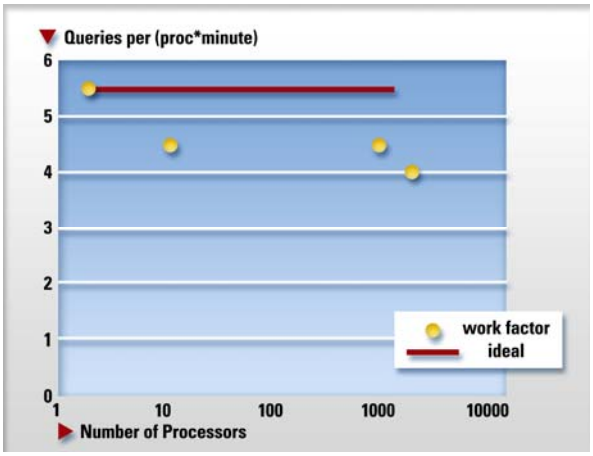

Figure 1. ScalaBLAST scalability

Citation

Oehmen CS and J Nieplocha. 2006. "ScalaBLAST: A Scalable Implementation of BLAST for High-Performance, Data-Intensive Bioinformatics Analysis." *IEEE Transactions on Parallel and Distributed Systems* 17(8):740-749.

High-Throughput Visual Analytics for Biological Sciences: Turning Data into Knowledge

CS Oehmen,[(a)] LA McCue,[(a)] JN Adkins,[(a)] KM Waters,[(a)] T Carlson,[(b)] WR Cannon,[(a)] BJ Webb-Robertson,[(a)] DJ Baxter,[(b)] ES Peterson,[(a)] M Singhal,[(a)] A Shah,[(a)] and KR Klicker [(a)]
(a) Pacific Northwest National Laboratory, Richland, Washington
(b) W.R. Wiley Environmental Molecular Sciences Laboratory, Richland, Washington

A diverse team of researchers collaborated on an entry for the International Conference for High-Performance Computing, Networking, Storage, and Analysis (SC 06) Analytics Challenge and was named one of the top three finalists. The final competition will take place in November at the SC 06 meeting in Tampa, Florida.

For the SC 06 Analytics Challenge, we have demonstrated an end-to-end solution for processing data produced by high-throughput, mass spectrometry (MS)-based proteomics. This approach, which allows biological hypotheses to be explored, is based on a tool called the Bioinformatics Resource Manager (BRM). BRM will interact with high-performance architectures and experimental data sources to provide high-throughput analytics to specific

experimental datasets. Peptide identification is achieved by a specially developed, data-intensive version of Polygraph, which has been shown to scale well beyond 1000 processors. Visual analytics applications, such as PQuad or Cytoscape, may be used to visualize protein identities in the context of pathways using data from public repositories such as the Kyoto Encyclopedia of Genes and Genomes. The end result is that a user can go from experimental spectra to pathway data in a single workflow, thereby reducing the time-to-solution for analyzing biological data from weeks to minutes. To view the video included with the PNNL/EMSL entry go to mms://ims4.pnl.gov/winmedia/2006/BRM/brm.wmv.

Scientific Grand Challenge Highlights

Isolation of a High-Affinity Functional Protein Complex between OmcA and MtrC: Two Outer Membrane Decaheme *c*-Type Cytochromes of *Shewanella oneidensis* MR-1

L Shi,[(a)] B Chen,[(a)] Z Wang,[(a)] DA Elias,[(a)] M Uljana Mayer,[(a)] YA Gorby,[(a)] S Ni,[(a)] BH Lower,[(a)] DW Kennedy,[(a)] DS Wunschel,[(a)] HM Mottaz,[(b)] MJ Marshall,[(a)] EA Hill,[(a)] AS Beliaev,[(a)] JM Zachara,[(a)] JK Fredrickson,[(a)] and TC Squier[(a)]
(a) Pacific Northwest National Laboratory, Richland, Washington
(b) W.R. Wiley Environmental Molecular Sciences Laboratory, Richland, Washington

A protein complex implicated in the reduction of manganese and iron was purified and its subunits identified. Identifying these proteins and their metal reduction capabilities is important for understanding bacterial physiology and facilitating bioremediation of contaminated sites, because the metal-reducing capability may also apply to toxic metals such as uranium, technetium, and chromium.

As a facultative anaerobic bacterium, *Shewanella oneidensis* MR-1 is able to use different forms of iron [Fe(III)] and manganese [Mn(III/IV)] as terminal electron acceptors during anaerobic respiration. Because Fe(III) and Mn(III/IV) are highly insoluble under neutral pH, *S. oneidensis* MR-1 cells have developed a sophisticated network that transports electrons from the cytoplasmic membrane, where electrons are generated, to the cell surface, where the reduction is thought to occur. C-type cytochromes are the major components of the electron transport network of *S. oneidensis* MR-1 that contains 39 putative c-type cytochromes. Located at outer membrane, MtrC and OmcA, which are two putative decaheme c-type cytochromes, are required for efficient reduction of Fe (III) and Mn (IV) by *S. oneidensis* MR-1. Despite the essential roles played by MtrC and OmcA in metal reduction, it is unclear if either

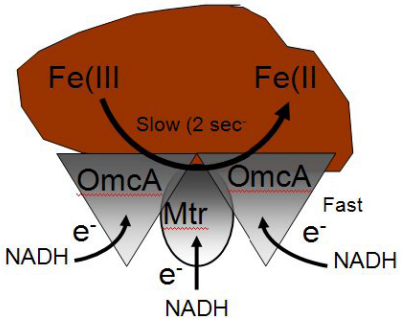

Figure 1. Model of protein complex between OmcA and MtrC. Oligomeric complex involving outer membrane (OM) decaheme cytochromes OmcA and MtrC permits coupling between NADH and reduction of Fe^{+3}. Rates of metal reduction are rate limiting (2 sec^{-1}), as evidenced by the virtually identical rate constants obtained from direct measurements of OmcA or MtrC oxidation relative to that associated with the NADH-dependent reduction of Fe(III)-NTA.

protein can directly reduce metals, or if they interact with other heme proteins or redox-active metabolites to reduce metal oxides.

To clarify the roles of MtrC and OmcA, we purified MtrC and OmcA. Each purified cytochrome contained tens of hemes and exhibited Fe(III)-NTA reductase activity. Endogenous MtrC also co-purifies with tagged OmcA in wild-type *Shewanella*, suggesting a direct association. To measure binding, we labeled MtrC with the multiuse affinity probe 4', 5'-bis(1,3,2-dithioarsolan-2-yl) fluorescein (1,2-ethanedithiol)$_2$, which specifically associates with a tetracysteine motif engineered at the C-terminus of MtrC. Upon titration with OmcA, we observed a marked increase in the fluorescence polarization indicating the formation of a high-affinity protein complex (K_d <500 nM) between MtrC and OmcA whose binding was sensitive to changes in ionic strength. Following association, we found that the MtrC/OmcA complex had an enhanced Fe(III)-NTA reductase-specific activity relative to either protein alone, thereby demonstrating that MtrC and OmcA can interact directly to form a stable complex that is consistent with their role in the electron-transport pathway of *S. oneidensis* MR-1.

Identification of the interaction between MtrC and OmcA and characterization of their capability to reduce metals contribute significantly to our understanding of bacterial physiology and to facilitating bioremediation of contaminated sites, because these metal-reducing activities may also function in the reduction and immobilization of toxic metals, including U(VI), Tc(VII), and Cr(VI).

The computational work has been performed by EMSL's J Li using pilot project emsl3227a sponsored by the Molecular Sciences Computing Facility (MSCF). The research was supported by the U.S. National Science Foundation and performed at EMSL.

Citations

Cui LF, X Huang, LM Wang, DY Zubarev, AI Boldyrev, J Li, and LS Wang. 2006a. "Sn_{12}^{2-}: Stannaspherene." *Journal of the American Chemical Society* 128(26):8390-8391.

Cui LF, X Huang, LM Wang, J Li, and LS Wang. 2006b. "Pb_{12}^{2-}: Plumbaspherene." *Journal of Physical Chemistry A* 110(34):10169-10172.

EMSL Grand Challenge Offers Insight into Uranium Bioremediation

MJ Marshall,[(a)] AS Beliaev,[(a)] A Dohnalkova,[(b)] DW Kennedy,[(a)] L Shi,[(a)] Z Wang,[(a)] MI Boyanov,[(c)] B Lai,[(c)] KM Kemner,[(c)] JS Mclean,[(a)] SB Reed,[(a)] DE Culley,[(a)] VL Bailey,[(a)] CJ Simonson,[(a)] D Saffarini,[(d)] MF Romine,[(a)] JM Zachara,[(a)] and JK Fredrickson[(a)]

(a) Pacific Northwest National Laboratory, Richland, Washington
(b) W.R. Wiley Environmental Molecular Sciences Laboratory, Richland, Washington
(c) Argonne National Laboratory, Argonne, Illinois
(d) University of Wisconsin, Milwaukee, Wisconsin

A research team studying the mechanisms of electron transport to metals and radionuclides by Shewanella oneidensis MR-1 has found that the outer membrane c-type cytochromes play an important role in uranium nanoparticle formation. This work is a significant advance in understanding radionuclide-reduction mechanisms.

A team of researchers from PNNL, the University of Wisconsin, and Argonne National Laboratory used the high-resolution electron microscopy facility at EMSL as part of the

Biogeochemical Grand Challenge project to address the microbial reduction of highly mobile uranium(VI) to a poorly soluble form called uraninite ($U(IV)O_2$). These researchers are studying the mechanisms of electron transport to metals and radionuclides by *Shewanella oneidensis* MR-1. They showed that outer membrane c-type cytochromes (i.e., proteins involved in electron transport or reductive/oxidative reactions) play a crucial role in biogenic UO_2 nanoparticle formation and extracellular localization with an extracellular polymeric substance (EPS). This research project is the first study to directly localize the outer membrane-associated cytochromes with EPS, as a complex structure, which contains UO_2 nanoparticles. While the exact mechanisms leading to the formation of UO_2-EPS matrix are yet to be determined, the UO_2 association with EPS clearly affects the nature and distribution of reduced uranium. In the environment, such association of UO_2 nanoparticles with biopolymers may exert a strong influence on subsequent behavior in the environment including susceptibility to oxidation by oxygen or transport in soils and sediments. Their work is a significant advance in understanding radionuclide-reduction mechanisms and the complex nature of the EPS associated with extracellular UO_2 nanoparticles (Marshall et al. 2006).

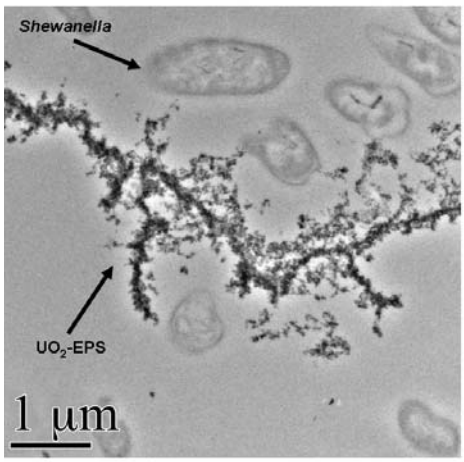

Figure 1. High-resolution transmission electron microscope image of *S. oneidensis* MR-1 incubated with uranium. Soluble U(VI) has been converted to nanoparticulate uraninite ($U(IV)O_2$) found in close association with complex extracellular polymeric substance secreted by the *Shewanella*.

The work is a part of a concentrated effort to characterize the biogeochemical processes involved in energy metabolism of metal and radionuclide contamination. It was supported by BER's Environmental Remediation Science and Genomics: GTL Programs. A portion of the work was performed as part of a Scientific Grand Challenge project at EMSL. Work at the Advanced Photon Source was supported by the DOE Office of Science, Office of Basic Energy Sciences. General user support for the x-ray fluorescence microprobe work was also provided by the DOE's Environmental Remediation Sciences Division.

Citation

Marshall MJ, AS Beliaev, AC Dohnalkova, DW Kennedy, L Shi, Z Wang, MI Boyanov, B Lai, KM Kemner, JS McLean, SB Reed, DE Culley, VL Bailey, CJ Simonson, DA Saffarini, MF Romine, JM Zachara, and JK Fredrickson. 2006. "C-Type Cytochrome-Dependent Formation of U(IV) Nanoparticles by *Shewanella oneidensis*." *PLoS Biology* 4(8):1324-1333. doi:10.13701/journal.pbio.0040268

Awards and Recognition

Yanwen Zhang

EMSL Staff Member Receives a 2005 Presidential Early Career Award for Scientists and Engineers. In July, Y Zhang, an EMSL materials physicist, was notified that she had been chosen to receive a 2005 Presidential Early Career Award for Scientists and Engineers, the highest honor bestowed by the U.S. government on outstanding scientists and engineers who are beginning their independent careers. Zhang and 55 other recipients were honored by President Bush and received their awards from John Marburger, director of the White House Office of Science and Technology Policy. The award recognizes scientists and engineers who show exceptional potential for leadership in scholarship, service, and education.

To be eligible for the presidential award, Zhang first had to be selected by DOE for its Early Career Scientist and Engineer Award. As a Presidential Early Career Award recipient, Zhang receives a commitment from DOE's Office of Science to continue funding the research for which the award was given for 5 years.

Zhang's research focuses on interactions of energetic ions with solid materials and how those interactions can be applied to the analysis and study of those materials. Zhang developed a novel way of measuring the energy loss of atomic particles as they pass through materials. Accurate measurements of such energy loss were a long-standing problem until Zhang successfully used high-resolution, time-of-flight spectroscopy to determine energy loss over a continuous range of energies.

With more than 100 publications and several long-term international research collaborations, Zhang is recognized for her contributions in ion-solid interactions, irradiation effects, and ion-beam techniques. She also is active in several professional societies, has received many international scientific and academic awards, and is involved in educational activities and community service. She routinely hosts visiting scientists at EMSL's ion-beam user facility; lectures on topics related to ion-beam physics; mentors postdoctoral fellows, graduate students, summer undergraduates, and high school interns; serves on Ph.D. committees; assists local middle schools with Chinese translations; and serves as a judge for local science fairs.

Zhang holds two doctorate degrees—one in engineering physics from Lund University in Sweden and another in science from Beijing Normal University in China.

GA Kimmel

EMSL User Featured in *Chemical and Engineering News*. EMSL user GA Kimmel was featured in the September 26, 2006, issue of *Chemical and Engineering News*. Kimmel was one of 200 scientists from around the world who attended a Nuclear Energy Workshop held by the U.S. Department of Energy to identify key areas of science in which fundamental research has the potential to make a significant impact on the future of nuclear power.

Professional/Community Service

Nothing reported.

Major Facility Upgrades

Confocal Raman microscope

Two major capabilities were made available to EMSL users through the Environmental Spectroscopy and Biogeochemistry Facility: 1) a confocal Raman spectrometer for the analysis of radiological samples, and 2) a single-crystal diffractometer.

The Raman spectrometer is a confocal Dilor XY 800, which is a high-resolution, modular triple spectrometer that can be operated in high-resolution or high-throughput modes, with both bulk sample and confocal microscopic capabilities. This Raman instrument is both a research grade triple spectrometer designed to provide a high degree of flexibility for bulk solid and liquid samples and a confocal microscope that can be used for spatially resolved analysis. It is anticipated that the greatest demand from EMSL users will be for confocal Raman microscopy, which has had significant impact in almost every field of the physical and chemical sciences. In the field of geosciences, confocal Raman spectroscopy allows extremely accurate spatial resolution in the x-y plane as well as depth profiling without distorting the spectral resolution. The instrument is located in the 331 Building Radiological Buffer Area in the 300 Area of DOE's Hanford Site. In this location, significant quantities of radioactive materials and diverse radionuclides can be investigated. Research of this type has included the investigation of the effects of radiation damage in ^{238}Pu-substituted silicates as potential radioactive waste storage materials, characterization of novel uranium mineral phases, characterization of contaminated soils from the Hanford Site, and identification of technetium-carboxylate solution species.

Bruker Proteum single-crystal diffractometer

The single-crystal diffractometer is a Bruker Proteum rotating annode instrument that provides brillant copper radiation. Detection is by a large-format, charged-coupled device. This combination of source and detector makes the instrument ideal for determining the structure of very large biological molecules as part of the Structural Biology research program in the Biological Science Division. Recently, software for the instrument was upgraded so that "small-molecule" research (e.g., for determining the structures of inorganic compounds) also can be accomodated. The new instrument can provide extremely high-resolution measurements of defect structures and lattice strain as a function of composition that would not be possible on a diffractometer with molybdenum radiation. It also has a liquid nitrogen cooling stage for temperature-dependent measurements.

Nuclear Magnetic Resonance (NMR) Spectrometer. One of the marquee capabilities at EMSL is the 900-MHz NMR spectrometer. A key component of this instrument is the sample probe, which holds the sample, sends radio-frequency energy into the sample, and detects the signal emanating from the sample. A unique Varian bio-magic angle spinning (MAS) probe coupled to the 900-MHz NMR spectrometer has helped researchers demonstrate the first steps of structure determination of a small protein in the solid state. The experiments were performed on microcrystalline GB1—a streptococcal protein—at 900 MHz by PNNL researcher AS Lipton and C Rienstra, who is a chemistry professor at the University of Illinois and a member of the DOE BER Advisory Committee. Historically, researchers have long been unable to fully meet the challenge of determining the structures of membrane-bound proteins; however, the high resolution and "spectacular" spectra achieved using the probe/900-MHz system combination will help Rienstra address ambiguities encountered in similar data from experiments using 750- and 500-MHz systems. The probe/900-MHz system combination is the first of its type in existence—with very few bio-MAS probes linked to NMR systems at any field—and promises to create a new user base in structure determination research at EMSL.

Mass Spectrometry Capabilities Extended. A second "OrbitrapTM" mass spectrometer was delivered to the EMSL High-Performance Mass Spectrometry Facility and was installed in September. Final configuration of the spectrometer to operate with the nano-liquid chromatographs will occur in early October and the system will be integrated into production operations in the proteomics facility by the end of October. This addition is a significant contribution to building a unique world capability in high-precision, high-throughput analysis in proteomics that has the potential to revolutionize our understanding of biological processes by understanding how the translation of genomic information into proteins is regulated.

MPP2 Memory Upgrade. In September, the Molecular Sciences Computing Facility (MSCF) received new Random Access Memory (RAM) to upgrade the MPP2 supercomputer. All of the MPP2 nodes will be upgraded from 6 or 8 gigabytes of RAM to 10 gigabytes.

MSCF Tape Archive Moved to Permanent Home. EMSL's new robotic tape library was moved in September from a temporary location in the MSCF to its permanent home in the Applied Process Engineering Laboratory in Richland, Washington. The tape library has a capacity of 5000 high-capacity computer tapes, and is used to keep backup copies of valuable EMSL data.

NWChem Version 5.0 Released. Some of the major additions in the recently released Version 5 of NWChem include large improvements in time-to-solution for the high-accuracy TCE and CCSD(T) modules, full integration between molecular mechanics and quantum mechanical theories and properties, equation-of-motion CCSD(T) methods for large-scale calculations of singly and partial doubly excited states, availability of exact exchange and self-interaction correction in the plane wave module, addition of dynamic proton hopping (Q-HOP methodology from the University of Saarland, Germany) to the molecular dynamics module, and addition of an interface with VENUS, which is a chemical dynamics code from Texas Tech University. Details about NWChem, including a user's guide and download information, are located at http://www.emsl.pnl.gov/docs/nwchem/nwchem.html.

ECCE (Extensible Computational Chemistry Environment) Version 4.0 Released. ECCE is the graphical user interface that supports NWChem. ECCE 4.0 extends its support for NWChem into the field of molecular dynamics, providing full end-to-end support for this class of simulations. It includes cross-platform support (including Microsoft Windows and Macintosh OS X) by migrating several applications to a cross-platform open source user interface development toolkit.

New Computer Procurement. The HPCS3 procurement process to acquire a new supercomputer to replace the aging mpp2 has passed Gate 1, and the request for proposals for our next generation MSCF supercomputer is being developed.

News Coverage

BH Lower, along with collaborators S Lower, Ri Yongsunthon, E Alexander, and V Fowler Jr., were highlighted in a the "Current Topics" section of the September 2006 edition of the journal *Microbe* for work performed at EMSL. The "Current Topic" highlight, entitled, "Mighty Microbes: Bacterial Bonding Is Plenty Powerful," can be accessed at http://www.asm.org/microbe/index.asp?bid=44704.

Brian H. Lower

Visitors and Users

During this reporting period, a total of 372 users benefited from EMSL capabilities and the expertise of EMSL staff members. This total included 226 onsite users and 146 remote users.

New EMSL Staff

P Nichols has been hired as a postdoctoral fellow in the MSCF High-Performance Software Development group. He will focus on development of relativistic methodologies in NWChem and the application of these new capabilities to studies on oxidation states of actinide complexes.

Publications

Adkins JN, HM Mottaz, AD Norbeck, JK Gustin, J Rue, T Clauss, SO Purvine, KD Rodland, F Heffron, and RD Smith. 2006. "Analysis of the *Salmonella typhimurium* Proteome through Environmental Response toward Infectious Conditions." *Molecular & Cellular Proteomics. MCP* 5(8):1450-1461. doi:10.1074/mcp.M600139-MCP200

Bagus P, C Woll, and ES Ilton. 2006. "A Definitive Analysis of the Rydberg and Valence Anti-Bonding Character of States in the O K-edge of H_2O." *Chemical Physics Letters* 428(1-3):207-212. doi:10.1016/j.cplett.2006.07.030

Beck KM, M Henyk, CM Wang, PE Trevisanutto, PV Sushko, WP Hess, and AL Shluger. 2006. "Site-Specific Laser Modification of MgO Nanoclusters: Towards Atomic-Scale Surface Structuring." *Physical Review B. Chemical Matter and Materials Physcs* 74(4): Art. No. 045404.

Berben LA, FC Mary, NR Crawford, and J Long. 2006. "Angle-Dependent Electronic Effects in 4,4'-Bipyridine-Bridged Ru3 Triangle and Ru4 Square Complexes." *Inorganic Chemistry* 45(16):6378-6386.

Bernholdt DE, BA Allan, RC Armstrong, F Bertrand, K Chiu, TL Dahlgren, K Damevski, WR Elwasif, TG Epperly, M Govindaraju, DS Katz, JA Kohl, M Krishnan, GK Kumfert, J Larson, S Lefantzi, MJ Lewis, AD Malony, LC McInnes, J Nieplocha, B Norris, SG Parker, J Ray, S Shende, TL Windus, and S Zhou. 2006. "A Component Architecture for High-Performance Scientific Computing." *International Journal of High-Performance Computing Applications* 20(2):163-202.

Bickmore BR, KM Rosso, CJ Tadanier, EJ Bylaska, and D Doud. 2006. "Bond-Valence Methods for pKa Prediction. II. Bond-Valence, Electrostatic, Molecular Geometry, and Solvation Effects." *Geochimica et Cosmochimica Acta* 70(16):4057-4071.

Blake TA and SS Xantheas. 2006. "Structure, Vibrational Spectra, and Ring Puckering Barrier of Cyclobutane." *Journal of Physical Chemistry A* 110(35):10487-10494.

Boily J, J Szanyi, and AR Felmy. 2006. "A Combined FTIR and TPD Study on the Bulk and Surface Dehydroxylation and Decarbonation of Synthetic Goethite." *Geochimica et Cosmochimica Acta* 70(14):3613-3624.

Bondarchuk O, X Huang, J Kim, BD Kay, LS Wang, JM White, and Z Dohnalek. 2006. "Formation of Monodisperse $(WO_3)_3$ Clusters on $TiO_2(110)$." *Angewandte Chemie-International Edition* 45(29):4786-4789.

Brim H, JP Osborne, HM Kostandarithis, JK Fredrickson, LP Wackett, and MJ Daly. 2006. "*Deinococcus radiodurans* Engineered for Complete Toluene Degradation Facilitates Cr(VI) Reduction." *Microbiology* 152(8):2469-2477.

Buchko GW, CY Kim, TC Terwilliger, and MA Kennedy. 2006. "Solution Structure of the Conserved Hypothetical Protein Rv2302 from the Bacterium *Mycobacterium tuberculosis*." *Journal of Bacteriology* 188(16):5993-6001.

Callister SJ, M Dominguez, CD Nicora, X Zeng, C Tavano, S Kaplan, T Donohue, RD Smith, and MS Lipton. 2006. "Application of the Accurate Mass and Time Tag Approach to the Proteome Analysis of Sub-Cellular Fractions Obtained from *Rhodobacter sphaeroides* 2.4.1 Aerobic and Photosynthetic Cell Cultures." *Journal of Proteome Research* 5(8):1940-1947.

Cui LF, X Huang, LM Wang, J Li, and LS Wang. 2006. "Pb-12(2-): Plumbaspherene." *Journal of Physical Chemistry A* 110(34):10169-10172.

Cui LF, X Huang, LM Wang, DY Zubarev, AI Boldyrev, J Li, and LS Wang. 2006. "Sn_{12}^{2-}: Stannaspherene." *Journal of the American Chemical Society* 128(26):8390-8391.

Devanathan R, LR Corrales, WJ Weber, A Chartier, and C Meis. 2006. "Atomistic Simulation of Collision Cascades in Zircon." *Nuclear Instruments and Methods in Physics Research. Section B, Beam Interactions with Materials and Atoms* 250(1-2):46-49. doi:10.1016/j.nimb.2006.04.109

Diamond DL, S Proll, JM Jacobs, EY Chan, DG Camp, II, RD Smith, and MG Katze. 2006. "HepatoProteomics: Applying Proteomic Technologies to the Study of Liver Function and Disease." *Hepatology* 44(2):299-308.

Ding YR, KK Hixson, CS Giometti, A Stanley, A Esteve-Nunez, T Khare, S Tollaksen, W Zhu, JN Adkins, MS Lipton, RD Smith, T Mester, and DR Lovley. 2006. "The Proteome of Dissimilatory Metal-Reducing Microorganism *Geobacter sulfurreducens* under Various Growth Conditions." *Biochimica et Biophysica Acta--Proteins and Proteomics*. 1764(7):1198-1206.

Fernandez FM, VH Wysocki, JH Futrell, and J Laskin. 2006. "Protein Identification via Surface-Induced Dissociation in an FT-ICR Mass Spectrometer and a Patchwork Sequencing Approach." *Journal of the American Society for Mass Spectrometry* 17(5):700-709.

Fu YJ, J Laskin, and LS Wang. 2006. "Collision-Induced Dissociation of [4Fe-4S] Cubane Cluster Complexes: [Fe4S4Cl4-x(SC2H5)(x)](2-/1-) (x=0-4)." *International Journal of Mass Spectrometry* 255:102-110.

Gallagher NB, TA Blake, PL Gassman, JM Shaver, and W Windig. 2006. "Multivariate Curve Resolution Applied to Infrared Reflection Measurements of Soil Contaminated with an Organophosphorus Analyte." *Applied Spectroscopy* 60(7):713-722.

Gao F, R Devanathan, T Oda, and WJ Weber. 2006. "Development of Partial-Charge Potential for GaN." *Nuclear Instruments and Methods in Physics Research. Section B, Beam Interactions with Materials and Atoms* 250(1-2):50-53. doi:10.1016/j.nimb.2006.04.082

Gao F, Y Zhang, M Posselt, and WJ Weber. 2006. "Atomic-Level Simulations of Epitaxial Recrystallization and Amorphous-to-Crystalline Transition in 4H-SiC." *Physical Review B. Condensed Matter and Materials Physics* 74(10): Art. No. 104108, 1-9. doi:10.1103/PhysRevB.74.104108

Gu Z, JH Edgar, CM Wang, and D Coffey. 2006. "Thermal Oxidation of Aluminum Nitride Powder." *Journal of the American Ceramic Society* 89(7):2167–2171. doi:10.1111/j.1551-2916.2006.01065.x

Hughes M, D Nielsen, E Rosenberg, R Gobetto, A Viale, SD Burton, and JJ Ford. 2006. "Structural Investigations of Silica Polyamine Composites: Surface Coverage, Metal Ion Coordination, and Ligand Modification." *Industrial and Engineering Chemistry Research* 45(19):6538-6547.

Johnson TJ, T Masiello, and SW Sharpe. 2006. "The Quantitative Infrared and NIR Spectrum of CH212 Vapor: Vibrational Assignments and Potential for Atmospheric Monitoring." *Atmospheric Chemistry and Physics* 6(9):2581-2591.

Gorby YA, S Yanina, JS Mclean, KM Rosso, DM Moyles, A Dohnalkova, TJ Beveridge, I Chang, BH Kim, KS Kim, DE Culley, SB Reed, MF Romine, D Saffarini, EA Hill, L Shi, DA Elias, DW Kennedy, GE Pinchuk, K Watanabe, S Ishii, B Logan, KH Nealson, and JK Fredrickson. 2006. "Electrically Conductive Bacterial Nanowires Produced by *Shewanella oneidensis* Strain MR-1 and Other Microorganisms." *Proceedings of the National Academy of Sciences of the United States of America* 103(30):11358-11363.

Ibrahim YM, K Tang, AV Tolmachev, AA Shvartsburg, and RD Smith. 2006. "Improving Mass Spectrometer Sensitivity Using a High-Pressure Electrodynamic Ion Funnel Interface." *Journal of the American Society for Mass Spectrometry* 17(9):1299-1305. doi:10.1016/j.jasms.2006.06.005

Ilton ES, SM Heald, SC Smith, D Elbert, and C Liu. 2006. "Reduction of Uranyl in the Interlayer Region of Low Iron Micas under Anoxic and Aerobic Conditions." *Environmental Science & Technology* 40(16):5003-5009.

Jiang W, Y Zhang, WJ Weber, J Lian, and RC Ewing. 2006. "Direct Evidence of N Aggregation and Diffusion in Au+ Irradiated GaN." *Applied Physics Letters* 89(2):021903-1—021903-3.

Joensson CT, IA Maximov, HJ Whitlow, V Shutthanadan, LV Saraf, DE McCready, BW Arey, Y Zhang, and S Thevuthasan. 2006. "Synthesis and Characterization of Cobalt Silicide Films on Silicon." *Nuclear Instruments and Methods in Physics Research. Section B, Beam Interactions with Materials and Atoms* 249(1-2):532–535. doi:10.1016/j.nimb.2006.03.046

Joly AG, M Henyk, KM Beck, PE Trevisanutto, PV Sushko, WP Hess, and AL Shluger. 2006. "Probing Electron Transfer Dynamics at MgO Surfaces by Mg-Atom Desorption." *Journal of Physical Chemistry B* 110(37):18093-18096.

Kim J, H Jia, C Lee, S Chung, J Kwak, Y Shin, A Dohnalkova, B Kim, P Wang, and JW Grate. 2006. "Single Enzyme Nanoparticles in Nanoporous Silica: A Hierarchical Approach to Enzyme Stabilization and Immobilization." *Enzyme and Microbial Technology* 39:474-480.

Kimmel GA, NG Petrik, Z Dohnalek, and BD Kay. 2006. "Layer-by-Layer Growth of Thin Amorphous Solid Water Films on Pt(111) and Pd(111)." *Journal of Chemical Physics* 125(4): Art. No. 044713

Kukkadapu RK, JM Zachara, JK Fredrickson, JP McKinley, DW Kennedy, SC Smith, and H Dong. 2006. "Reductive Biotransformation of Fe in Shale-Limestone Saprolite Containing Fe(III) Oxides and Fe(II)/Fe(III) Phyllosilicates." *Geochimica et Cosmochimica Acta* 70(14):3662-3676.

Laskin J. 2006. "Energetics and Dynamics of Fragmentation of Protonated Leucine Enkephalin from Time- and Energy-Resolved Surface-Induced Dissociation Studies." *Journal of Physical Chemistry A* 110(27):8554-8562.

Laskin A, H Wang, WH Robertson, JP Cowin, MJ Ezell, and BJ Finlayson-Pitts. 2006. "A New Approach to Determining Gas-Particle Reaction Probabilities and Application to the Heterogeneous Reaction of Deliquesced Sodium Chloride Particles with Gas-Phase Hydroxyl Radicals." *Journal of Physical Chemistry A* 110(36):10619-10627.

Liu G, J Wang, S Lea, and Y Lin. 2006. "Bioassay Labels Based on Apoferritin Nanovehicles." *Chembiochem* 7(9):1315-1319. doi:10.1002/cbic.200600225

Liu RC, DH Hu, X Tan, and HP Lu. 2006. "Revealing Two-State Protein-Protein Interactions of Calmodulin by Single-Molecule Spectroscopy." *Journal of the American Chemical Society* 128(31):10034-10042.

Liu T, W Qian, HM Mottaz, MA Gritsenko, AD Norbeck, RJ Moore, SO Purvine, DG Camp, II, and RD Smith. 2006. "Evaluation of Multi-Protein Immunoaffinity Subtraction Systems for Plasma Proteomics and Candidate Biomarker Discovery Using Mass Spectrometry." *Molecular & Cellular Proteomics*. doi:10.1074/mcp.T600039-MCP200

Liu YF, W Chen, AG Joly, YQ Wang, C Pope, YB Zhang, JO Bovin, and P Sherwood. 2006. "Comparison of Water-Soluble CdTe Nanoparticles Synthesized in Air and in Nitrogen." *Journal of Physical Chemistry B* 110(34):16992-17000.

Lumetta GJ, BK McNamara, TL Hubler, DW Wester, J Li, and SL Latesky. 2006. "Potential Application of Kläui Ligands in Actinide Separations." In *Separations for the Nuclear Fuel Cycle in the 21st Century*, pp. 201-218, American Chemical Society, Washington, D.C.

Maki A, JKG Watson, T Masiello, and TA Blake. 2006. "Observation of a Forbidden E"-A'_1 Infrared Transition in $^{11}BF_3$." *Journal of Molecular Spectroscopy* 238(2):135-144.

Marshall MJ, AS Beliaev, A Dohnalkova, DW Kennedy, L Shi, Z Wang, MI Boyanov, B Lai, KM Kemner, JS Mclean, SB Reed, DE Culley, VL Bailey, CJ Simonson, D Saffarini, MF Romine, JM Zachara, and JK Fredrickson. 2006. "c-Type Cytochrome-Dependent Formation of U(IV) Nanoparticles by *Shewanella oneidensis*." *PloS Biology* 4(8):1324-1333.

Minard KR, DR Einstein, RE Jacob, S Kabilan, AP Kuprat, C Timchalk, LL Trease, and RA Corley. 2006. "Application of Magnetic Resonance (MR) Imaging for the Development and Validation of Computational Fluid Dynamic (CFD) Models of the Rat Respiratory System." *Inhalation Toxicology* 18(10):787-794. doi: 10.1080/08958370600748729

Nie J, HY Xiao, X Zu, and F Gao. 2006. "First-Principles Study of Sb Adsorption on Ag (110)(2×2)." *Chemical Physics* 326(2-3):583-588.

Nie L, G Wu, FJ Brockman, and W Zhang. 2006. "Integrated Analysis of Transcriptomic and Proteomic Data of *Desulfovibrio vulgaris*: Zero-Inflated Poisson Regression Models to Integrate and Interpret Microarray and Proteomic Data." *Bioinformatics* 22(13):1641-1647. doi:10.1093/bioinformatics/btl134

Oehmen CS and J Nieplocha. 2006. "ScalaBLAST: A Scalable Implementation of BLAST for High-Performance, Data-Intensive Bioinformatics Analysis." *IEEE Transactions on Parallel and Distributed Systems* 17(8):740-749.

Petritis K, LJ Kangas, B Yan, EF Strittmatter, ME Monroe, W Qian, JN Adkins, RJ Moore, Y Xu, MS Lipton, DG Camp, II, and RD Smith. 2006. "Improved Peptide Elution Time Prediction for Reversed-Phase Liquid Chromatography-MS by Incorporating Peptide Sequence Information." *Analytical Chemistry* 78(14):5026-5039.

Punnoose A, MH Engelhard, and JS Hays. 2006. "Dopant Distribution, Oxygen Stoichiometry and Magnetism of Nanoscale $Sn_{0.99}Co_{0.01}$." *Solid State Communications* 139(8):434-438. doi:10.1016/j.ssc.2005.09.040

Raugei S and P Carloni. 2005. "Structure and Function of Vanadium Haloperoxidases." *Journal of Physical Chemistry B* 110:3747-3758.

Redington RL, TE Redington, and RL Sams. 2006. "Quantum Tunneling in the Midrange Vibrational Fundamentals of Tropolone." *Journal of Physical Chemistry A* 110(31):9633-9642.

Roh Y, H Gao, H Vali, DW Kennedy, Z Yang, W Gao, A Dohnalkova, RD Stapleton, J Moon, TJ Phelps, JK Fredrickson, and J Zhou. 2006. "Metal Reduction and Iron Biomineralization by a Psychrotolerant Fe(III)-Reducing Bacterium, *Shewanella sp.* Strain PV-4." *Applied and Environmental Microbiology* 72(5):3236-3244. doi:10.1128/AEM.72.5.3236-3244.2006

Sacksteder CA, W Qian, TV Knyushko, HH Wang, MH Chin, DG Camp, II, RD Smith, D Smith, TC Squier, and DJ Bigelow. 2006. "Endogenously Nitrated Proteins in Mouse Brain: Links to Neurodegenerative Disease." *Biochemistry* 45(26):8009-8022.

Sacksteder CA, JE Whittier, Y Xiong, J Li, NA Galeva, ME Jacoby, SO Purvine, TD Williams, MC Rechsteiner, DJ Bigelow, and TC Squier. 2006. "Tertiary Structural Rearrangements upon Oxidation of Methionine145 in Calmodulin Promotes Targeted Proteasomal Degradation." *Biophysical Journal* 91(4):1480-1493.

Schmitt S, H Prokisch, T Schlunk, DG Camp, II, U Ahting, T Waizenegger, CM Scharfe, T Meitinger, A Imhof, W Neupert, PJ Oefner, and D Rapaport. 2006. "Proteome Analysis of Mitochondrial Outer Membrane from *Neurospora crassa*." *Proteomics* 6(1):72-80. doi:10.1002/pmic.200402084

Shi L, B Chen, Z Wang, DA Elias, MU Mayer, YA Gorby, S Ni, BH Lower, DW Kennedy, DS Wunschel, HM Mottaz, MJ Marshall, EA Hill, AS Beliaev, JM Zachara, JK Fredrickson, and TC Squier. 2006. "Isolation of High-Affinity Functional Protein Complex between OmcA and MtrC: Two Outer Membrane Decaheme c-type Cytochromes of *Shewanella oneidensis* MR-1." *Journal of Bacteriology* 188(13):4705-4714. doi:10.1128/JB.01966-05 Grand Challenge

Shi L, JN Adkins, JR Coleman, AA Schepmoes, A Dohnalkova, HM Mottaz, AD Norbeck, SO Purvine, NP Manes, HS Smallwood, HH Wang, J Forbes, P Gros, S Uzzau, KD Rodland, F Heffron, RD Smith, and TC Squier. 2006. "Proteomic Analysis of *Salmonella enterica Serovar Typhimurium* Isolated from RAW 264.7 Macrophages: Identification of a Novel Protein that Contributes to the Replication of *Serovar typhimurium* Inside Macrophages." *Journal of Biological Chemistry* 281:29131-29140.

Simner SP, MD Anderson, MH Engelhard, and JW Stevenson. 2006. "Degradation Mechanisms of La-Sr-Co-Fe-O_3 SOFC Cathodes." *Electrochemical and Solid-State Letters* 9(10):A478-A481.

Simson DC, S Ahn, L Pasa-Tolic, B Bogdanov, HM Mottaz, AN Vilkov, GA Anderson, MS Lipton, and RD Smith. 2006. "Using Size Exclusion Chromatography-RPLC and RPLC-CIEF as Two-Dimensional Separation Strategies for Protein Profiling." *Electrophoresis* 27(13):2722-2733. doi:10.1002/elps.20060003

Smith DM, KM Rosso, M Dupuis, M Valiev, and T Straatsma. 2006. "Electronic Coupling between Heme Electron-Transfer Centers and Its Decay with Distance Depends Strongly on Relative Orientation." *Journal of Physical Chemistry B* 110(31):15582-15588.

Stewart ML, AL Ward, and DR Rector. 2006. "A Study of Pore Geometry Effects on Anisotropy in Hydraulic Permeability Using the Lattice-Boltzmann Method." *Advances in Water Resources* 29(9):1328-1340.

Sturdy YK, C Skylaris, and DC Clary. 2006. "Torsional Anharmonicity in the Conformational Analysis of β-D-Galactose." *Journal of Physical Chemistry B* 110:3485-3492.

Su F, Y Liu, W Chen, WJ Wang, K Ding, G Li, AG Joly, and DE McCready. 2006. "Temperature and Pressure Dependences of the Copper-Related Green Emission in ZnO Microrods." *Journal of Applied Physics* 100(1):013107-1—013107-6. doi:10.1063/1.2206705

Tanimura K, E Inami, J Kanasaki, and WP Hess. 2006. "Two-Hole Localization Mechanism for Electronic Bond Rupture of Surface Atoms by Laser-Induced Valence Excitation of Semiconductors." *Physical Review B. Condensed Matter and Materials Physics* 74(3): Art. No. 035337.

Thompson CJ, RG Riley, JE Amonette, and PL Gassman. 2006. "Quantification of Volatile Organics in Soil Aging Experiments using Fourier Transform Infrared Spectroscopy." *Applied Spectroscopy* 60(8):914-919.

Tonkyn RG, RS Disselkamp, and CHF Peden. 2006. "Nitrogen Release from a NOx Storage and Reduction Catalyst." *Catalysis Today* 114(1):94-101.

Wander MC, SN Kerisit, KM Rosso, and MA Schoonen. 2006. "Kinetics of Triscarbonato Uranyl Reduction by Aqueous Ferrous Iron: A Theoretical Study." *Journal of Physical Chemistry A* 110(31):9691-9701.

Wang J, G Liu, and Y Lin. 2006. "Electroactive Silica Nanoparticles for Biological Labeling." *Small* 2(10):1134-1138.

Wang J, Q Lu, and HP Lu. 2006. "Single-Molecule Dynamics Reveals Cooperative Binding-Folding in Protein Recognition." *PLoS Computational Biology* 2(7):842-852.

Wang XB, HK Woo, X Huang, MM Kappes, and LS Wang. 2006. "Direct Experimental Probe of the On-Site Coulomb Repulsion in the Doubly Charged Fullerene Anion C-70 (2-)." *Physical Review Letters* 96(14): Art. No. 143002

Wang XB, HK Woo, LS Wang, B Minofar, and P Jungwirth. 2006. "Determination of the Electron Affinity of the Acetyloxyl Radical (CH_3COO) by Low-Temperature Anion Photoelectron Spectroscopy and *Ab Initio* Calculations." *Journal of Physical Chemistry A* 110(15):5047-5050.

Wang Z, AR Felmy, Y Xia, and EC Buck. 2006. "Observation of Aqueous Cm(III)/Eu(III) and UO22+ Nanoparticulates at Concentrations Approaching Solubility Limit by Laser-Induced Fluorescence Spectroscopy." *Journal of Alloys and Compounds* 418(1-2):166-170.

Waters T, XB Wang, HK Woo, and LS Wang. 2006. "Photoelectron Spectroscopy of the Bis(dithiolene) Anions [M(mnt)(2)](n-)(M = Fe-Zn; n=1, 2): Changes in Electronic Structure with Variation of Metal Center and with Oxidation." *Inorganic Chemistry* 45(15):5841-5851.

Wu Q and T Van Voorhis. 2006. "Direct Calculation of Electron Transfer Parameters through Constrained Density Functional Theory." *Journal of Physical Chemistry A* 110(29):9212-9218.

Xantheas SS and TA Blake. 2006. "Structure, Vibrational Spectra and Ring Puckering Barrier of Cyclobutane." *Journal of Physical Chemistry A* 110:10487-10494.

Xiong G, AG Joly, GR Holtom, CM Wang, DE McCready, KM Beck, and WP Hess. 2006. "Excited Carrier Dynamics of α-Cr_2O_3/α-Fe_2O_3 Core-Shell Nanostructures." *Journal of Physical Chemistry B* 110(34):16937-16940. doi:10.1021/jp062507n S1520-6106(06)02507-7

Yadav NN, S Maheswaran, V Shutthanandan, S Thevuthasan, TR Hart, H Ngo, and S Vigneswaran. 2006. "Comparison of Analytical Techniques for Analysis of Arsenic Adsorbed on Carbon." *Water Quality Research Journal of Canada* 41(2):185-189.

Zhang L, M DeRider, MA McCornack, C Jao, N Isern, T Ness, R Moyer, and PJ LiWang. 2006. "Solution Structure of the Complex Between Poxvirus-Encoded CC Chemokine Inhibitor vCCI and Human MIP-1β" *Proceedings of the National Academy of Sciences of the United States of America* 103(38): 13985-13990.

Zhang W, MA Gritsenko, RJ Moore, DE Culley, L Nie, K Petritis, EF Strittmatter, DG Camp, II, RD Smith, and FJ Brockman. 2006. "A Proteomic view of *Desulfovibrio vulgaris* Metabolism as Determined by Liquid Chromatography Coupled with Tandem Mass Spectrometry." *Proteomics* 6(15):4286-4299. doi:10.1002/pmic.200500930

Zhang Y, WJ Weber, V Shutthanandan, and S Thevuthasan. 2006. "Non-linear Damage Accumulation in Au-Irradiated $SrTiO_3$." *Nuclear Instruments and Methods in Physics Research. Section B, Beam Interactions with Materials and Atoms* 251(1):127-132. doi:10.1016/j.nimb.2006.05.018

Zhang Y, WJ Weber, DA Grove, J Jensen, and G Possnert. 2006. "Electronic Stopping Powers for Heavy Ions in Niobium and Tantalum Pentoxides." *Nuclear Instruments and Methods in Physics Research. Section B, Beam Interactions with Materials and Atoms* 250(1-2):62-65. doi:10.1016/j.nimb.2006.04.148

Zhang Y, J Jensen, G Possnert, DA Grove, DE McCready, BW Arey, and WJ Weber. 2006. "Electronic Stopping Forces of Heavy Ions in Metal Oxides." *Nuclear Instruments and Methods in Physics Research. Section B, Beam Interactions with Materials and Atoms* 249(1-2):18-21. doi:10.1016/j.nimb.2006.03.013

Presentations

During this reporting period, EMSL staff presented papers on research performed at the user facility at the following meetings or locations.

- American Chemical Society National Meeting and Exposition, September 2006, San Francisco, California.
- International Aerosol Conference 2006, August 2006, St. Paul, Minnesota.

Patents

None reported.

Journal Covers

LS Wang, EMSL user from PNNL, and his collaborators have discovered a new class of endohedreal lead cage compounds that they have named "plumbaspherenes" (see research highlight entitled "Pb_{12}^{2-}: Plumbaspherene"). The existence of these new cage compounds may allow for the insertion of other atoms inside these cages to create new materials with unique properties for a wide range of applications. This research was featured on the cover of the August 31, 2006, issue of the *Journal of Physical Chemistry A*.